AIP Journal of Applied Physics

Structural origin of the relaxor-to-normal ferroelectric transition in Pb (Mg 1/3 Nb 2/3 O 3) – x Pb Ti O 3

Hu Cao, Jiefang Li, and D. Viehland

Citation: Journal of Applied Physics **100**, 034110 (2006); doi: 10.1063/1.2219164
View online: http://dx.doi.org/10.1063/1.2219164
View Table of Contents: http://scitation.aip.org/content/aip/journal/jap/100/3?ver=pdfcov
Published by the AIP Publishing

Structural origin of the relaxor-to-normal ferroelectric transition in $Pb(Mg_{1/3}Nb_{2/3}O_3)-xPbTiO_3$

Hu Cao,[a] Jiefang Li, and D. Viehland
Department of Materials Science and Engineering, Virginia Tech, Blacksburg, Virginia 24061

(Received 10 November 2005; accepted 25 May 2006; published online 9 August 2006)

A relaxor-to-normal, or micro-to-macrodomain, transition in $Pb(Mg_{1/3}Nb_{2/3}O_3)-xPbTiO_3$, has been found under electric fields applied along [001] for $x \geqslant 0.24$. It is shown that an intermediate tetragonal ferroelectric phase is important to the sharpness of this transition, as observed in its dielectric response. © *2006 American Institute of Physics*. [DOI: 10.1063/1.2219164]

I. INTRODUCTION

In the zero-field-cooled (ZFC) condition, the complex perovskite $Pb(Mg_{1/3}Nb_{2/3})O_3$ (PMN) is a relaxor ferroelectric, whose characteristic feature is a large dielectric permittivity that is strongly frequency dispersive.[1] This dielectric anomaly does not have a corresponding structural phase transition, as the average symmetry remains cubic until very low temperature.[2,3] Diffuse neutron scattering has been observed on cooling below 600 K,[3–6] indicating a local polarization, consistent with prior electron microscopy studies that have shown polar nanoregions (PNR's).[7,8] Short-range atomic shifts have been found by diffuse neutrons to become static below a characteristic temperature, which is less than that of the dielectric maximum (T_M).[3] In the solid solution PMN–xPbTiO$_3$ (PMN–xPT), the substitution of Ti^{4+} on the B site results in a macroscopic ferroelectric phase with average symmetry changes near T_M. A spectrum of structures and a variety of macroscopic properties can be "tuned" by Ti^{4+} substitution, ranging from a pseudocubic (C) in the relaxor state to ferroelectric rhombohedral (R), monoclinic (M), and tetragonal (T) phases near the morphotropic phase boundary (MPB) for $0.31 < x < 0.37$.[9]

In the field-cooled (FC) condition, the phase stability and properties of PMN–x%PT are dramatically altered,[10] relative to the ZFC. A normal ferroelectric state is induced by electric field (E), which has micron-sized domains and a remnant polarization. Structural studies by x rays and neutrons have shown a complicated phase stability that is dependent on electric history, in particular, in the vicinity of the MPB. Various monoclinic (M_A and M_C) phases have been reported for E applied along the $(001)_C$.[9–12] As can be seen in Fig. 1, crystals of PMN–0.30PT are R in the ZFC condition, but M_A in the FC condition;[11] whereas PMN–0.35PT is monoclinic M_C in both the ZFC and FC conditions.[9,12] Property investigations of both ZFC and FC PMN–xPT have also previously been performed. For $x < 0.30$, application of E also results in a significant change in the permittivity.[13] An abrupt micro-to-macrodomain transition has been reported in the related relaxor system $Pb_{(1-x)}La_x(Zr_{0.65}Ti_{0.35})_{1-x/4}O_3$ ($x = 0.8$) (PLZT 8/65/35) in the FC condition.[14] Subsequent investigations of tetragonal PLZT 12/40/60 revealed a spontaneous relaxor-to-normal transition in the ZFC condition,[15] where a large c/a change of the T phase was believed to be crucial to the sharpness of the transition.

Interestingly, in the PMN–xPT diagram of Fig. 1, the stability of an intermediate T phase field can be seen to be shifted to lower PT contents by application of $E \| (001)$. In the FC condition for $0.24 < x < 0.30$, this intermediate T phase is stable over a narrow temperature, bridging the cubic (C) and M phases. This is notably different from the ZFC condition, where the transitional sequence is $C \rightarrow R$. In this letter, we will show the importance of this intermediate T phase on triggering the sharpness of a relaxor-to-normal transition in field-cooled $(001)_c$ PMN–xPT crystals for $0.24 < x < 0.30$.

II. EXPERIMENTAL PROCEDURE

Single crystals of (001)-oriented PMN–0.24PT and PMN–0.28PT with dimension of $3 \times 3 \times 3$ mm^3 were obtained from HC Materials (Urbana, IL) and were polished

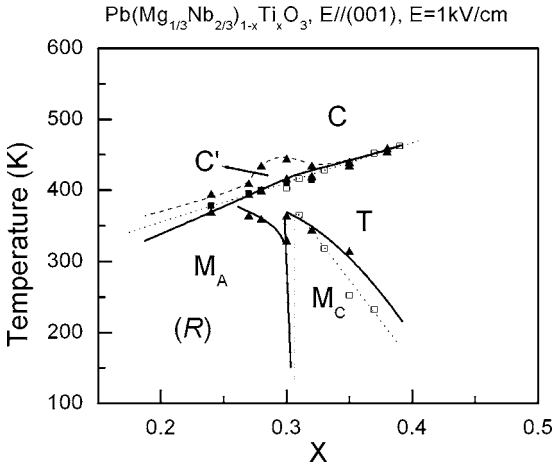

FIG. 1. Modified phase diagram of PMN–xPT as a function of $E \| (001)$. The dotted lines and open square signs were based on the prior studies by Noheda *et al.* (Ref. 9). The phases in the zero-field-cooled (ZFC) state are indicated by italics font. The solid square signs represent T_M determined by dielectric measurments. The solid curves drawn through these triangular data points are only to guide the eyes. The upper dashed curve represents the limite of the cubic phase (C) determined by an abnormal thermal expansion that occurs on cooling into a distorted cubic phase field (designated as C'). The solid curve at lower temperatures indicates where the stability limit of the ferroelectric phase.

[a]Electronic mail: hcao@vt.edu

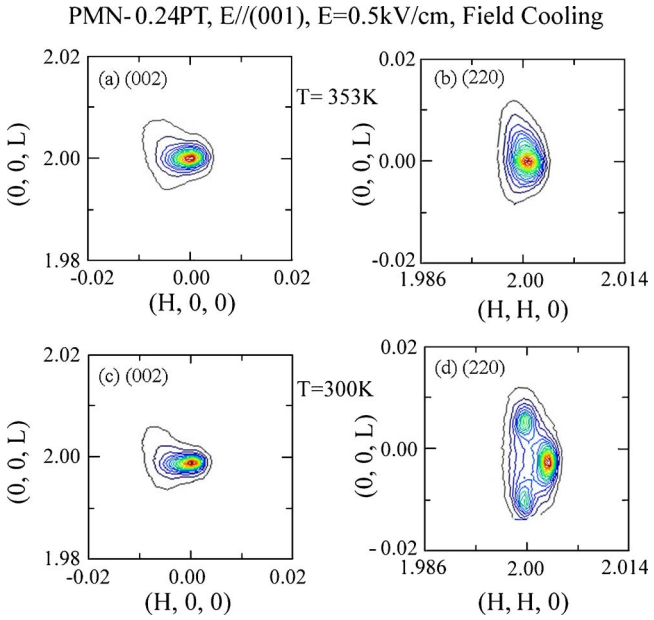

FIG. 2. The mesh scans around (002) and (220) reflections at 353 and 300 K for PMN–0.24PT as E=0.5 kV/cm in FC condition.

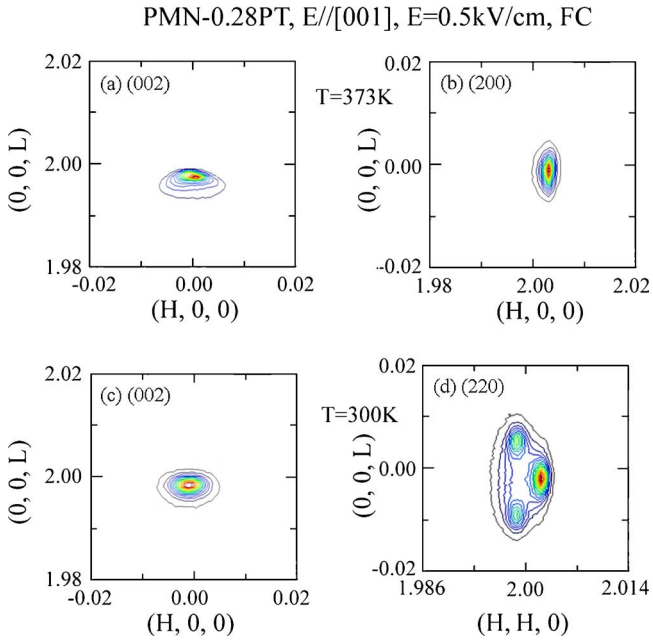

FIG. 3. The mesh scans for PMN–0.28PT as E=0.5 kV/cm in FC condition, (a) around (002) and (200) reflections at 373 K and (b) around (002) and (220) reflections at 300 K.

using 0.25 μm alpha alumina. Gold electrodes were deposited on one pair of opposite (001) faces of the cube by sputtering. Temperature dependent dielectric constant measurements were performed using a multifrequency *LCR* meter (HP 4284A) under various $E\|(001)$. The x-ray diffraction (XRD) studies were performed using a Philips MPD high-resolution system equipped with a two bounce hybrid monochromator, an open three-circle Eulerian cradle, and a doomed hot stage. A Ge (220)-cut crystal was used as an analyzer, which had an angular resolution of 0.0068°. The x-ray wavelength was that of Cu $K\alpha$=1.5406 Å, and the x-ray generator operated at 45 kV and 40 mA. Each measurement cycle was begun by heating up to 550 K to depole the crystal, and measurements subsequently taken on cooling. In this study we fixed the reciprocal lattice unit (or 1 r.l.u.) $a^*=2\pi/a=1.560$ Å^{-1}. All mesh scans of PMN–xPT shown in this study were plotted in reference to this reciprocal unit.

III. RESULTS AND DISCUSSION

To obtain a compressive picture of the PMN–0.24PT structural properties in the FC condition we took mesh scans around the (002), (200), and (220) at 423, 353, and 300 K as E=0.5 kV/cm, as shown in Fig. 2. PMN–0.24PT has a $C \rightarrow M_A$ sequence in the FC state with $E\|[001]$.

(a) At 423 K, the (002) and (200) mesh scans did not exhibit splitting (data not shown here), and it was found that $a=c$. Thus, it is clear that the lattice is cubic

(b) With decreasing temperature to 353 K, the mesh scans around the (002) and (220) reflections [Figs. 2(a) and 2(b)] remain as a single peak. It was observed that the lattice parameter c determined from the (002) reflection is slightly larger than lattice parameter a determined from the (200) reflection. However, a tetragonal structure was not directly observed. Rather, this structure is pseudocubic; where the slight increase of c and decrease of a are presumed to be associated with the growth of microdomains under applied E.

(c) With further decreasing temperature, a M_A phase was found to appear at 338 K. As given in Figs. 2(c) and 2(d) at 300 K, the contour maps exhibit only a single peak around the (002) reflection, revealing that the c axis is fixed along the direction that E is applied. The contour map around the (220) reflection shows three peaks, i.e., (220) twin peaks and one $(2\bar{2}0)$ peak: the c axis is fixed, but there exits multiple domains that are twinned about the [110].

Figure 3 shows the mesh scans for PMN–0.28PT taken about the (002), (200), and (220) under E=0.5 kV/cm applied along [001] at temperatures of 373 and 300 K. For $E\|[001]$, PMN–0.28PT has a $C \rightarrow T \rightarrow M_A$ sequence in the FC state. In Figs. 3(a) and 3(b), the mesh scans taken about the (002) and (200) exhibit only a single peak at 373 K; indicating that a T phase was induced by E, whose lattice parameters are a=4.021 Å and c=4.034 Å. With decreasing temperature, the (002) and (220) mesh scans at 300 K revealed the same domain configurations as that of the M_A phase of PMN–0.24PT.

Figure 4 shows the corresponding lattice parameters as a function of temperature under E=0.5 kV/cm for (a) PMN–0.24PT and (b) PMN–0.28PT. For both crystals, the (002) and (200) reflections did not exhibit any splitting at temperatures greater than T_M. Thus, it is clear that both are cubic in this temperature range, with $a \approx c$. On cooling in the C phase, the a_C lattice parameter, as derived from the (002) reflection, decreased linearly with decreasing temperature. In the vicinity of T_M of the respective crystals, an abnormal positive thermal expansion was observed in the lattice parameter with decreasing temperature. No other evidence of

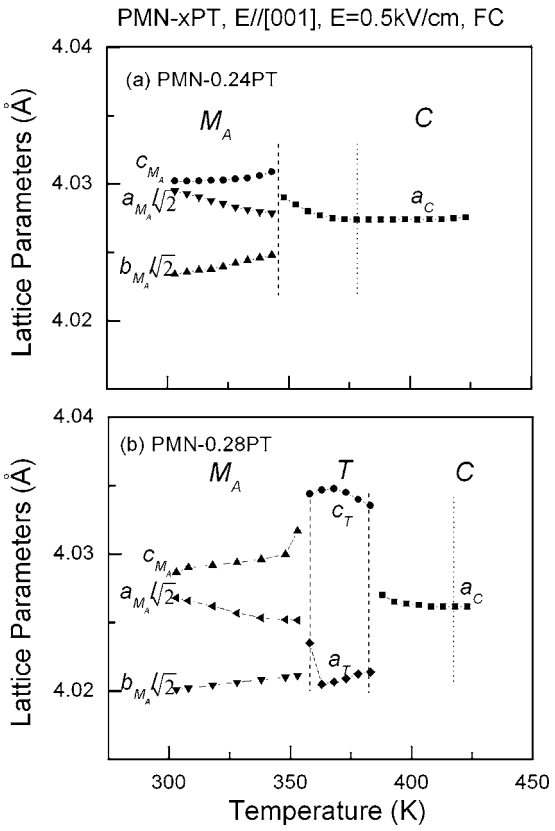

FIG. 4. Temperature dependence of the lattice parameters under $E=0.5$ kV/cm applied along [001] for (a) PMN–0.24PT and (b) PMN–0.28PT.

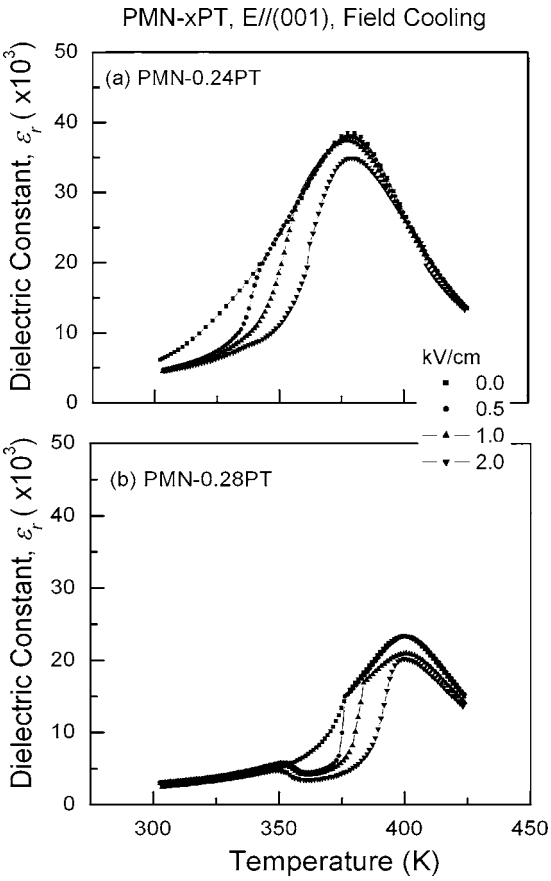

FIG. 5. Temperature dependence of the dielectric constant (1 kHz) under various electric fields for (a) PMN–0.24PT and (b) PMN–0.28PT.

peak splitting was observed. For PMN–0.24PT, with further decreasing temperature, a $C \rightarrow M_A$ transition occurred at 340 K; where the value of c_M exhibited a sharp increase, and that of $a_M/\sqrt{2}$ and $b_M/\sqrt{2}$ a sharp decrease. For PMN–0.28PT an intermediate T phase was found between 382 and 358 K, which subsequently transformed to M_A at 358 K.

Figure 5 shows the dielectric constant ($f=1$ kHz) as a function of temperature under $E \| [001]$ for (a) PMN–0.24PT and (b) PMN–0.28PT. The ZFC dielectric behavior of both crystals exhibited a broad peak, typical of relaxor ferroelectrics. However, the FC dielectric behaviors are quite different. For PMN–0.24PT ($T_M=378$ K), the dielectric constant decreased sharply upon application of $E=0.5$ kV/cm at 342 K. Under $E=2$ kV/cm, it is noteworthy that a sharp drop in the dielectric constant was observed near 360 K, and that a secondary less pronounced dielectric anomaly was found near 340 K. For $E=2$ kV/cm, mesh scans (not shown) revealed a pseudocubic structure (c is close to but larger than a) between 378 and 340 K; whereas at temperatures lower than 340 K, mesh scans revealed a M_A one. Accordingly, in reference to prior phase diagram studies,[9] we believe that tetragonality in PMN–0.24PT is present over a narrow temperature range: where the sharp drop in dielectric constant corresponds to a relaxor→tetragonal transition, and the secondary smaller anomaly to a $T \rightarrow M_A$ one. Whereas, for PMN–0.28PT ($T_M=400$ K), the dielectric behavior under $E=0.5$ kV/cm exhibited a sharp decrease near 376 K, indicating a relaxor-to-normal ferroelectric transition. With decreasing temperature, a secondary phase transition was found at ~350 K. Mesh scans revealed that PMN–0.28PT had a T structure below 376 K, and a M_A one below the secondary dielectric maximum of 350 K. Comparisons of the results in Figs. 4 and 5 will show a correspondence of (i) the relaxor-to-normal transition with an intermediate T phase in PMN–0.24PT and PMN–0.28PT, where the $C \rightarrow T$ boundary shifts to higher temperatures with increasing E; and (ii) a secondary transition for PMN–0.28PT, and a small anomaly in the dielectric constant for PMN–0.24PT at 2 kV/cm with a transition to a M_A phase.

Next, in Fig. 6, we present the temperature dependence of the $d_{(002)}$ lattice parameter under various E for FC PMN–0.28PT. A sharp $C \rightarrow T$ transition can be seen at lower fields of $E \leqslant 1$ kV/cm. However, with increasing E, the transition became increasingly gradual, and the $C \rightarrow T$ boundary harder to delineate. These findings are consistent with the dielectric results of Fig. 5 that show the relaxor-to-normal transition becoming increasingly broad with E. Comparison of the structural and dielectric data demonstrates the importance of a significant c/a change on the sharpness of the relaxor-to-normal transition.

The relaxor-to-normal ferroelectric phase transition has previously been explained by interactions between PNR's, which are strong enough to provoke ferroelectric-type ordering below T_M. Structural evolution can be considered in three steps. First, near T_B (Burns temperature), clusters of short-range polar order (i.e., PNR's) gradually increase in number and grow on cooling. Second, with decreasing temperature,

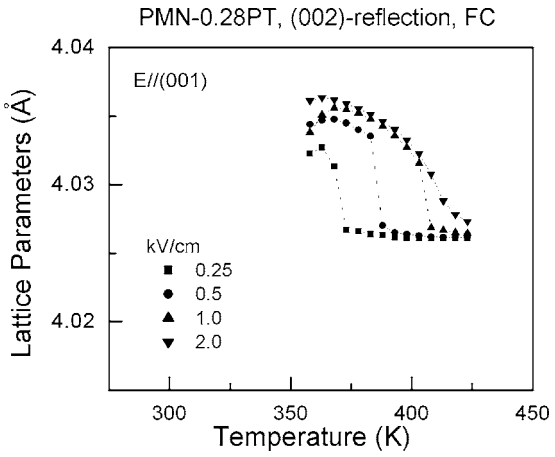

FIG. 6. Lattice parameter derived from the (002)-reflection as a function of tepmerature for PMN–0.28PT under various levels of $E\|(001)$.

the ensemble of PNR's becomes percolating, resulting in abnormal thermal expansion near T_M, as can been in Fig. 3; application of E then aligns these PNR's. Third, below T_M, a field-forced structural phase transition occurs from the PNR ensemble condition to abnormal ferroelectric state—this transition is first orderlike, and once induced is stable on further cooling. Previous investigations reported that the relaxor-to-normal transition was spontaneous in tetragonal relaxor systems, whereas rhombohedral ones possessed such abrupt changes only in the FC condition.[11,14,15] It was argued that the large c/a ratio of the tetragonal structure was the driving force triggering the spontaneity, whereas systems with smaller c/a ratios (such as rhombohedral) could only undergo a field-forced transition. However, our findings here provide a better unifying structural basis for a relaxor-to-normal transition: a tetragonal structure is required in all cases. For PMN–xPT, the lack of a spontaneous transition in the ZFC condition is due to a sequence that does not proceed through a tetragonal phase. For example, the dielectric behaviors of PMN–0.24PT and PMN–0.28PT did show a smoothly varying curve below T_M. However, on field cooling under a small field of $E=0.5$ kV/cm, the transformational sequence was altered, and an intermediate T structure present over a narrow temperature range for both PMN–0.24PT and PMN–0.28PT. The expression of a fully formed tetragonal phase is seemingly critical to the sharpness of the relaxor-to-normal transition.

In summary, for PMN–xPT with $x>0.24$, our investigation shows the correspondence of (i) an intermediate T phase with a sharp relaxor-to-normal transition and (ii) a significant decrease of the dielectric constant at the relaxor-normal ($C' \rightarrow T$) transition, and a secondary dielectric anomaly upon transforming to the M_A phase. The results demonstrate that the structural origin of the sharp transitional nature of a relaxor-to-natural transition is the presence of an intermediate tetragonal phase.

ACKNOWLEDGMENTS

The authors would like to gratefully acknowledge financial support from the Office of Naval Research under Grant Nos. N000140210340 and N000140210126 and MURI N0000140110761.

[1]L. E. Cross, Ferroelectrics **151**, 305 (1994).
[2]P. Bonneau, P. Garnier, E. Husson, and A. Morell, Mater. Res. Bull. **24**, 201 (1989).
[3]N. de Mathan, E. Husson, G. Calvarin, J. R. Gavarri, A. W. Hewat, and A. Morell, J. Phys.: Condens. Matter **3**, 8159 (1991).
[4]P. Bonneau, P. Garnier, E. Husson, J. R. Gavarri, A. W. Hewat, and A. Morell, J. Solid State Chem. **91**, 350 (1991).
[5]Y. Useu, H. Tazawa, K. Fijishiro, and Y. Yamada, J. Korean Phys. Soc. **29**, S703 (1996).
[6]K. Fujishiro, T. Iwase, Y. Useu, Y. Yamada, B. Dkhil, J.-M. Kiat, S. Mori, and N. Yamamoto, J. Phys. Soc. Jpn. **69**, 2331 (2000).
[7]D. Viehland, M. Kim, Z. Xu, and J. F. Li, Appl. Phys. Lett. **67**, 2471 (1995).
[8]Z. Xu, M. Kim, J. F. Li, and D. Viehland, Philos. Mag. A **74**, 395 (1996).
[9]B. Noheda, Z. Zhong, D. E. Cox, G. Shirane, S. E. Park, and P. Rehrig, Phys. Rev. B **66**, 054104 (2002).
[10]H. Cao, F. Bai, J. Li, D. Viehland, G. Xu, H. Hiraka, and G. Shirane, J. Appl. Phys. **97**, 1 (2005).
[11]F. Bai, N. Wang, J. Li, D. Viehland, P. Gehring, G. Xu, and G. Shirane, J. Appl. Phys. **96**, 1620 (2004).
[12]J. Kiat, Y. Uesu, B. Dkhil, M. Matsuda, C. Malibert, and G. Calvarin, Phys. Rev. B **65**, 064106 (2002).
[13]G. Xu, D. Viehland, J. F. Li, P. M. Gehering, and G. Shirane, Phys. Rev. B **68**, 212410 (2003).
[14]Y. Xi, C. Zhili, and L. E. Cross, J. Appl. Phys. **54**, 3399 (1983).
[15]X. Xai, Z. Xu, and D. Viehland, Philos. Mag. B **70**, 33 (1994).